

# Pulsed electrodeposition and magnetism of two-dimensional assembly of controlled-size Co particles on Si substrates

M.V. Rastei<sup>\*</sup>, S. Colis, R. Meckenstock, O. Ersen, J.P. Bucher

*Institut de Physique et Chimie des Matériaux, Université Louis Pasteur, UMR 7504, 23 rue du Loess, BP 43, F-67034 Strasbourg Cedex 2, France*

Received 19 January 2006; accepted for publication 7 March 2006

Available online 29 March 2006

## Abstract

We present an extremely simple and inexpensive way to obtain controlled-size and density Co metallic particles on Si(1 1 1) using electrodeposition. When unpatterned substrates are used, the particle density and size can be controlled by adjusting the pulse frequency and the total deposition time. Randomly arranged cobalt particles with diameters of few tens of nanometres are obtained for short deposition times. Continuing the deposition, the particle size and density can be increased until coalescence. Magnetic force microscopy images show magnetically coupled/uncoupled particles depending on the size and distance between them. For small decoupled particles, no in-plane uniaxial anisotropy is found, in agreement with transmission electron microscopy observations which show randomly oriented single crystal particles. As the particle coalescence increases, the in-plane anisotropy evaluated from magnetization loops increases as well. When deposited on focused ion beam patterned substrates, well organized nanoparticles with adjustable magnetic anisotropy are obtained. Ferromagnetic resonance measurements performed on these samples reveal that the magnetic anisotropy originates mainly from the particle shape.

© 2006 Elsevier B.V. All rights reserved.

*Keywords:* Metal–semiconductor thin films structures; Magnetic nanoparticles; Pulsed electrodeposition

## 1. Introduction

The morphology, structure and magnetic properties of small metallic particles present an increased interest due to their potential applications in the field of magnetic recording and magneto-electronics. In most cases specific magnetic properties are required which can be obtained by controlling the particle size, density and shape. An interesting and delicate issue in the field of magnetism is to understand how these parameters influence the magnetic properties in such systems. From the experimental point of view, a simple method of growing and arranging metallic particles is of vital importance.

Electrodeposition is one of the most attractive techniques in many areas needing metal deposition. This fact

is mostly due to its low cost but also to the fact that it allows the growth of high aspect ratio structures like nanowires [1], pillars [2,3], well-organized nanoparticles [4–6], or metal/semiconductor Schottky barriers [7]. The processes involved in electrodeposition are quite well understood nowadays, but many aspects related to the early stage of the metal electrodeposition, especially on semiconductor surfaces, are still under investigation. It is generally found that electrodeposition on semiconductor starts from surface defects and that the growth itself follows a Volmer–Weber mode [6,8–17].

In this work, we present a simple and inexpensive way to grow metallic nanoparticles with controlled-size and density on patterned and unpatterned Si(1 1 1) using pulsed electrodeposition. First, we show that the particle size and the density in the randomly arranged nanoparticles deposited on unpatterned substrates can be modified by varying the total deposition time and the pulse frequency applied during growth. Second, we show that the particle

<sup>\*</sup> Corresponding author. Tel.: +33 388107021.

E-mail address: [rastei@ipcms.u-strasbg.fr](mailto:rastei@ipcms.u-strasbg.fr) (M.V. Rastei).

random nucleation on pre-existing defects can be avoided if one generates focused ion beam (FIB) patterned structures. This induces the growth of organized nanoparticles on well defined arrays. For each system the morphologic and magnetic properties including anisotropy and local magnetic correlations between particles are discussed.

## 2. Experimental details

Negatively doped Si (111) substrates with a resistivity of  $\sim 0.1 \Omega \text{ cm}$ , were first cleaned in sonically agitated acetone and washed several times with ultra-pure water. The back side of the substrate was electrically contacted and then covered by an insulating varnish in order to delimit at the front side a  $3 \times 3 \text{ mm}^2$  area for electrochemical deposition. The native silica layer was etched in 5% HF solution and then the pure Si was immediately transferred into the electrodeposition cell.

The electrochemical deposition was performed using a solution of  $\text{CoSO}_4$  (0.1 M) +  $\text{CoCl}_2$  (0.1 M) +  $\text{H}_3\text{BO}_3$  (0.64 M) with a pH of about 3.4. This mixed sulphate–chloride electrolyte assures a completely random crystallographic orientation of the grains [18], which is especially important in the case of organized particles. In this case the shape anisotropy imposed by the FIB pattern's shape has a stronger effect on the magnetization state of the particles. The reference electrode was  $\text{Hg}/\text{Hg}_2\text{SO}_4$  and a Pt wire was used as counter electrode. The electrodeposition of cobalt was carried out in galvanostatic mode by applying a duty cycle (50% on and 50% off) of 1, 3, and 5 Hz. The cycle off-time corresponds to zero current in the cell, while during the on-time, the galvanostat was set to deliver a constant current density of about  $-0.5 \text{ mA}/\text{cm}^2$ . This current value was set low enough to avoid hydrogen generation. Such phenomena can lead to uncovered areas on the substrate surface which can strongly influence the magnetic properties of the sample.

The topography of the deposits was investigated using a Nanoscope Dimension 3100 atomic force microscope (AFM) working in tapping mode. The local magnetism of the deposits was investigated by means of magnetic force microscopy (MFM), which allows the visualization of the magnetic domain structure and the magnetic correlations between the particles. As MFM probe, a commercially available silicon pyramidal tip coated with a 50 nm thick CoCr layer was used. The tip was magnetized along its axis in “down” direction (perpendicular to the sample plane) using a strong magnetic field of about 3 kOe.

The average magnetism was investigated using an alternating gradient field magnetometer (AGFM) [19]. The magnetization loops were recorded by applying the magnetic field parallel and perpendicular to the film surface in order to estimate the deposit anisotropy. In the case of organized particles on the FIB patterned substrates, due to the limited number of particles (about 62500), the anisotropy analysis was performed with a more sensitive technique: ferromagnetic resonance (FMR). These

measurements were performed in a standard X-band microwave cavity. The technique gives information on the anisotropy distribution of the samples in the saturated state [20]. By analyzing the resonance line position as a function of the external magnetic field magnitude and direction, it is possible to find the easy magnetization axis. This magnetization axis corresponds to the lowest line position in the FMR spectrum, since in this direction the magnetic moments are easier to saturate. The FMR measurements were performed at room temperature in a field comprised between 0 and 300 mT.

Transmission electron microscopy (TEM) observations were performed using a TOPCON 002B microscope operating at 200 kV. Small quantities of Co nanoparticles/Si were removed by scraping the substrate and then dispersed on a copper grid covered with an amorphous carbon membrane. The samples were investigated in high resolution transmission microscopy (HRTEM) mode.

## 3. Results and discussion

### 3.1. Randomly arranged nanoparticles

To obtain low-density Co nanoparticles, relatively short deposition times were used. In the Fig. 1 we show AFM (a), (b), (c) and the corresponding MFM (d), (e), (f) images taken on samples deposited for 12 s deposition time and for pulse frequencies of 1, 3 and 5 Hz, respectively. As expected for the weak silicon–cobalt ions interaction, the growth was performed in a 3D Volmer–Weber mode

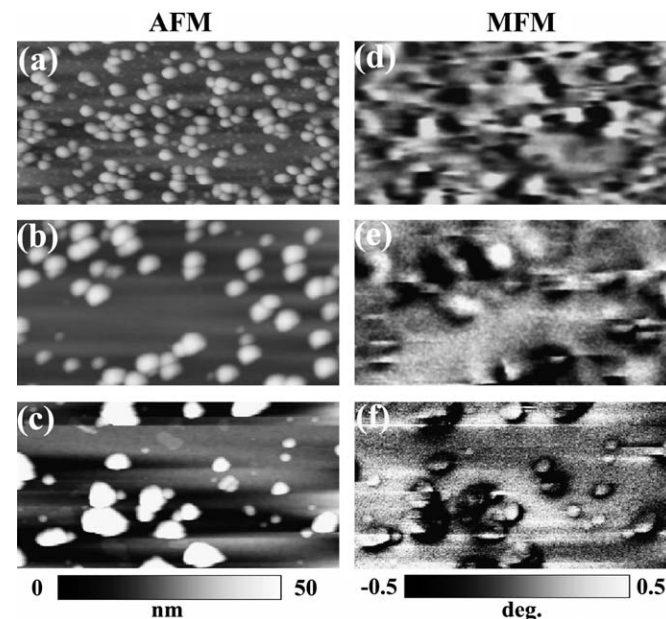


Fig. 1.  $1 \times 2 \mu\text{m}^2$  atomic force microscopy (AFM) (a)–(c) and the corresponding (d)–(f) magnetic force microscopy (MFM) images recorded on samples grown during 12 s. Different pulse frequencies were applied during growth: 1 Hz for sample (a), 3 Hz for sample (b), and 5 Hz for sample (c). No magnetic field was applied prior or during the MFM experiments.

on randomly distributed surface defects. Interestingly, a strong dependence of the particle density and size can be observed with respect to the pulse frequency applied during growth (see also Fig. 3), having strong influence on the magnetic correlations. A maximum density of about 100 particles/ $\mu\text{m}^2$  and small particle sizes, less than 30 nm, were obtained for the deposit performed at 1 Hz pulse frequency (Fig. 1(a)). We observed that the nucleation density increases when the pulse frequency decreases. This effect may be related to the shorter on/off deposition time (high pulse frequency), which limits the diffusion of Co ions on the Si surface. Additionally, the positive nucleation ramp in the beginning of the deposition process is only partly followed for each frequency pulse of the deposition sequence, for high pulse frequencies. Since during the on-time interval the number of the nuclei is enhanced, it is expected that low frequency duty cycles generate high particle densities. In contrast, for very low frequencies ( $<1$  Hz) the tendency is reversed due to the beginning of the diffusion limited growth during the on-time interval of the duty cycle.

The strong dark-bright dipole contrasts in the MFM image (Fig. 1(d)) reveals that many Co particles are magnetically coupled. Groups of such particles can be observed in both AFM and MFM images (Fig. 1). These high resolved MFM contrasts can be well observed by a carefully choice of the lift scan height. We found that the appropriate lift is 50 nm for the best MFM signal. The lateral resolution obtained by this approach is of about 15 nm, which is good enough to visualize if the particles are magnetically correlated, but also to investigate the magnetization state of a single particle. By increasing the pulse frequency at 3 Hz, the particle size increases and a strong decrease of the particle density is observed. Less particles are magnetically coupled due to the large distances between them. However, as noticed in the Fig. 1(b) and (e) even for these relatively large particles some magnetic correlations can be found, typically observed for coalesced particles. The deposition performed at 5 Hz produces particles up to 100 nm in diameter and density of only  $\sim 11$  particles/ $\mu\text{m}^2$ . In this case, no magnetic coupling was found by MFM measurements, as observed in Fig. 1(f).

Fig. 2(a)–(c) and (d)–(f) shows the AFM and MFM images for samples grown for 24 s deposition time, respectively. Much dense cobalt particles (see also Fig. 3) were obtained, with a slight increase of the particle size. Whereas the sample grown at 1 Hz reveals strong magnetic coupling between particles, much less magnetic correlations are observed for the samples grown at 3 and 5 Hz, due to the larger particle size. The strong correlations within the particle assembly made at 1 Hz during 24 s were evidenced by the in-plane large magnetic domains up to  $9 \times 10^4 \text{ nm}^2$  size. Such domains contain typically few tens of correlated Co particles. The in-plane orientation of the magnetization in these domains is due to the shape anisotropy which increases drastically when the particles become coalesced.

For 40 s deposition time and for all three pulse frequencies the Co particles are highly coalesced and the samples

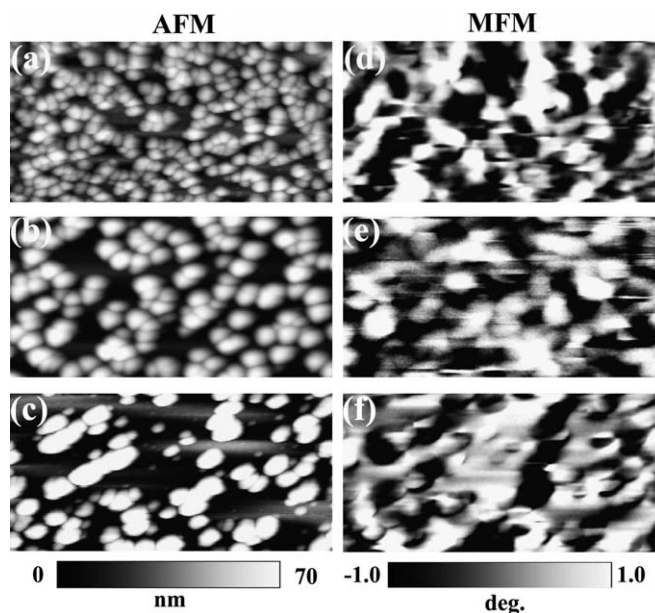


Fig. 2. Idem as Fig. 1, but for samples grown during 24 s.

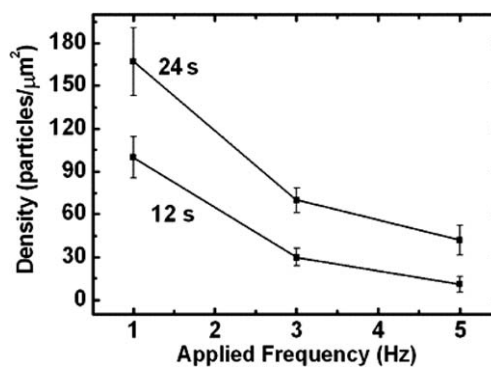


Fig. 3. The variation of the particle density for 12 s and 24 s deposition times as a function of pulse frequency applied during growth.

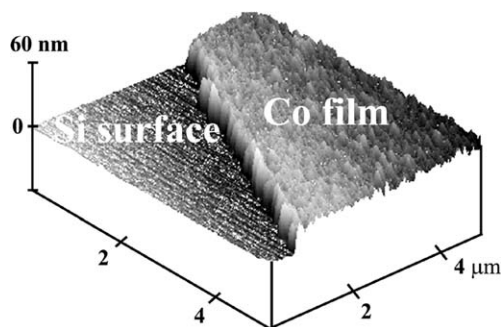


Fig. 4. AFM image taken on the film edge after the removing of the insulating varnish. For this sample the deposition time was 40 s and the pulse frequency 1 Hz.

can be considered as thin films. As an example we show in Fig. 4 an AFM image taken at the film edge. The film thickness can be easily measured after removing the insulating varnish. In this case homogeneous film thickness of  $\sim 30$  nm was measured in different edge areas of the sample.

For 3 and 5 Hz deposits, rougher films were obtained with thicknesses of about 40 and 50 nm, respectively. This slight increase of film thickness is due to the different rms error related to samples with a large particle size.

The in-plane magnetic anisotropy was measured by angle-dependent magnetization measurements. By rotating the samples in the film plane, no difference in magnetization curves was observed, indicating no in plane uniaxial anisotropy. This suggests that the particles have a randomly crystalline orientation.

In order to have an insight into the crystalline structure of the deposits, TEM observations have been performed. HRTEM images reveal a well defined crystalline structure of Co particles. Most of them are single crystals without stacking faults and other defects. Fig. 5 shows a HRTEM image of two adjacent nanoparticles scraped off from the sample imaged in Fig. 1(a). Within each particle a single crystal lattice can be observed, which consists of one set of lattice fringes with a spacing of 0.205 nm. This is consistent with the theoretical hcp {002} Co interplanar distance of 0.2035 nm. The *c* axes of two individual lattices, represented by white arrows in the figure, show the random orientation of two analyzed nanoparticles. Therefore, the absence of the uniaxial in-plane anisotropy of these samples can indeed be attributed to the random orientation of the single-crystal particles.

The magnetization measurements performed with the field applied perpendicular to the sample plane, reveal for all samples, larger saturation fields compared to those obtained in the in-plane configuration measurements, which speaks in favor of an in-plane anisotropy induced by the particle coalescence. For samples grown during 12 s, both in-plane and out-of-plane magnetization measurements reveal low values of remnant magnetization, which confirms the random orientation of the crystalline structure of the particles. The random character of the crystallographic axes seems to be maintained in all three space directions, as revealed by transmission electron microscopy and confirmed by a close inspection of the MFM images performed on single particles. To summarize the magnetization measurements, we plotted in Fig. 6 the effective anisotropy factor  $K_{\text{eff}}$  as a function of the deposition time. These variations show a continuous increase of  $K_{\text{eff}}$  with the deposi-

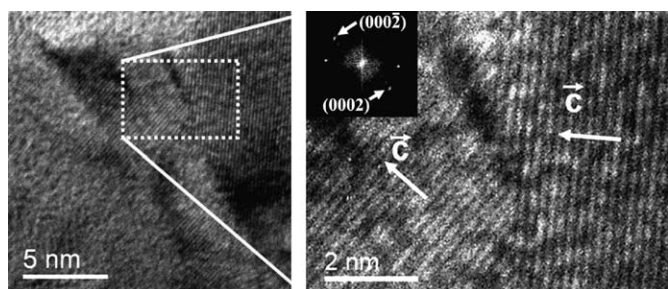


Fig. 5. TEM image reflecting the different orientation of the particle *c*-axes. The particles were scraped from the sample grown at 1 Hz pulse frequency and during 12 s.

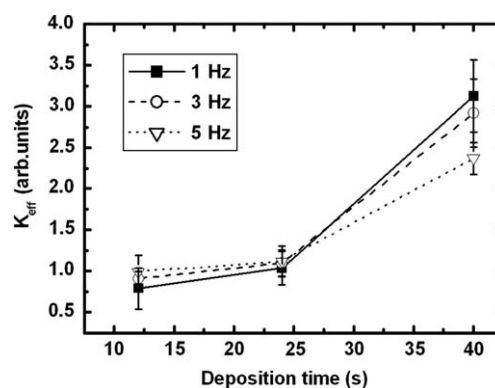


Fig. 6. The effective anisotropy  $K_{\text{eff}}$  as a function of the deposition time for samples grown at 1, 3 and 5 Hz pulse frequencies. The lines are only a guide for the eyes.

tion time, for all pulse frequencies, in agreement with the AFM images which show an increasing number of coalesced particles with the deposition time. Moreover, the significant increase of  $K_{\text{eff}}$  was observed for the deposits made at 1 Hz, indicating that the coalescence of these small particles increases significantly the in-plane anisotropy. In contrast,  $K_{\text{eff}}$  of the Co particles made using higher pulse frequencies (3 and 5 Hz) seems to be nearly unaffected up to 24 s deposition time, albeit the particle density increases. The drastic increase of  $K_{\text{eff}}$  with the further increase of the deposition time at 40 s is due to the formation of compact films. In this case, the reduction of the  $K_{\text{eff}}$  value with the increasing pulse frequency can easily be explained by the increased film thickness for high pulse frequency and by the reduced correlation between the large particles.

### 3.2. Organized nanoparticles

The random character of the Co particles nucleation on natural defects can be avoided by creating focused ion beam (FIB) small defects in the Si substrate, covered previously with a 200 nm thick  $\text{SiO}_2$  layer. Square arrays of holes, 400 nm deep and distant by  $2 \mu\text{m}$ , were etched on different substrates. As shown in the scanning electron microscopy (SEM) images of Fig. 7(a)–(c), three hole diameters (550, 400 and 200 nm) were chosen in order to investigate the effect of the particle shape on the magnetic properties.

AFM observations performed after the Co electrodeposition at a rate of 1 Hz, show that the holes are homogeneously filled and protrude by a maximum of 10 nm out of the surface (Fig. 7(d)–(f)). The current density and the deposition time were about  $-0.5 \text{ mA/cm}^2$  and 180 s, respectively. The deposition time presented limited variations from one sample to another due to the confined growth conditions. The choice of 1 Hz pulse frequency was revealed to be the most adequate to grow organized particles, since, as observed in the case of particle growth on free silicon surface, this pulse sequence assures the smallest grain size and the highest nucleation density. This

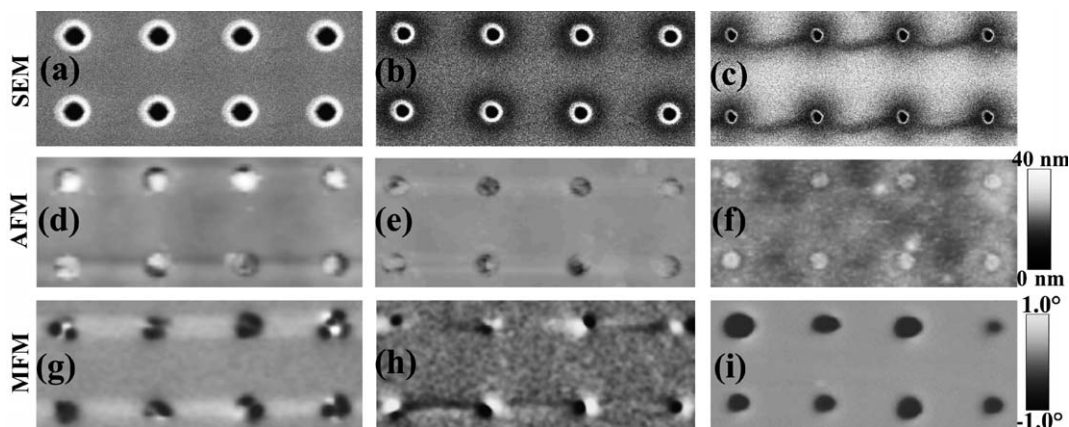


Fig. 7. (a)–(c) SEM images of FIB-etched holes with different geometries on SiO<sub>2</sub>/Si substrates. All holes are 400 nm deep and have diameters of 550, 400 and 200 nm, respectively. (d)–(f) AFM images taken after the electrodeposition of Co within the holes. (g)–(i) The MFM images recorded for the perpendicular “down” remnant state.

confirms a compact and homogeneous growth avoiding empty volumes or other defects inside the particle which can lead to a large magnetic properties distribution. We believe that the Co particles within the holes are made of crystalline grains randomly oriented. This is supported by AFM images that reveal a granular nature of the upper part of the Co particles.

To give an overview on the magnetic properties of the differently shaped Co particles from Fig. 7, FMR and MFM investigations were performed.

The Co particles with an aspect ratio of 0.7 have a multidomain structure, as shown by the MFM observations (Fig. 7(g)). This is in agreement with the in-plane to out-of-plane angle-dependent FMR measurements which show the lowest resonance line for the in-plane applied field of about 0.10 T as presented in Fig. 8. The large line width of the spectrum is due to the random crystalline distribution of the Co particles in the sample plane. The in-plane angle dependent FMR measurements do not reveal any difference in the resonance line position, confirming the random orientation of the magnetization from magnetic domains.

For particles with an aspect ratio of 1, the MFM measurements indicate a single domain state of the Co particles with a magnetization randomly distributed in the plane (Fig. 7(h)). This is confirmed by the FMR spectrum

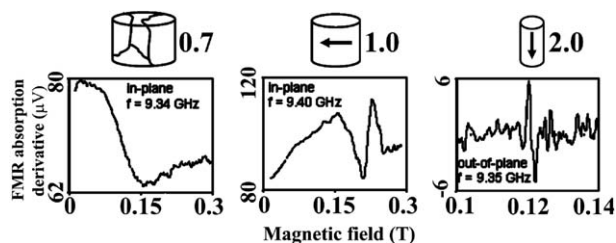


Fig. 8. FMR spectra of different aspect ratios Co nanoparticles (height/diameter of 0.7, 1.0, and 2.0) electrodeposited on FIB-structured Si substrates.

(Fig. 8). The shifted line position to higher resonant fields and the narrow width of the resonance peak show an increase of the shape anisotropy of the Co particles. The in-plane to out-of-plane angle-dependent FMR measurements show the lowest resonance line position at about 0.20 T for 9.4 GHz which clearly proves that the easy magnetization axes of the particles lie in the sample plane. Moreover, the in-plane angle-dependent FMR measurements show no in-plane uniaxial anisotropy.

The MFM experiments performed on the Co particles with an aspect ratio of 2 showed single domain states with the magnetization oriented perpendicular to the sample plane (Fig. 7(i)). As for the previous samples, this is in agreement with the FMR measurements given in the Fig. 8. In this case, the lowest resonance line position is found when the field is perpendicular to the sample plane, at about 0.12 T, and exhibits a narrow resonance, indicating that nearly all particles are in the same magnetic state with their easy magnetization axis strictly aligned along the particle axis.

#### 4. Conclusion

Frequency-dependent pulsed electrodeposition with an equal on- and off-times was used in order to produce controlled-size and density nanometric Co particles on Si (111) surface. The morphology, structure and magnetic properties of the Co nanoparticles were investigated. We found that for randomly distributed particles the magnetic anisotropy is dominated by the magnetic inter-grain correlations. MFM images indicated magnetically coupled/uncoupled particles depending on the distance between them. Small uncoupled particles are found to have no in-plane uniaxial anisotropy, in agreement with TEM observations which show randomly oriented single-crystal particles. The magnetization measurements showed that the in-plane magnetic anisotropy increases faster for small particles, when the particle density was increased.

The random particle nucleation on pre-existing defects was avoided by generating FIB patterned structures that induce the growth of organized nanoparticles. Furthermore, we show that a careful tuning of the dimensions of the FIB-etched defects, allows the adjustment of the magnetic anisotropy of the grown Co nanoparticles. MFM and FMR investigations indicated that the magnetization state was mainly induced by the Co nanoparticle shape.

## References

- [1] G.E. Possin, Rev. Sci. Instrum. 41 (1970) 772.
- [2] W. Xu, J. Wong, C.C. Cheng, R. Johnson, A. Scherer, J. Vac. Sci. Technol. B 13 (1995) 2372.
- [3] J. Wong, A. Scherer, M. Todorovic, S. Schultz, J. Appl. Phys. 85 (1999) 5489.
- [4] M.V. Rastei, R. Meckenstock, J.P. Bucher, E. Devaux, Th. Ebbsen, Appl. Phys. Lett. 85 (2004) 2050.
- [5] J. Carray, K. Bouzehouane, J.M. George, C. Ceneray, T. Blon, M. Bibes, A. Vaurès, S. Fusil, S. Kenane, L. Vila, L. Piraux, Appl. Phys. Lett. 81 (2002) 760.
- [6] M.L. Munford, F. Maroun, R. Cortes, P. Allongue, A.A. Pasa, Surf. Sci. 537 (2003) 95.
- [7] G. Oskam, D. van Heerden, P.C. Searson, Appl. Phys. Lett. 73 (1998) 3241.
- [8] G. Oskam, L. Bart, D. Vanmaekelbergh, J.J. Kelly, J. Appl. Phys. 75 (1993) 3238.
- [9] P. Allongue, E. Souteyrand, L. Allemand, J. Electroanal. Chem. 362 (1993) 89.
- [10] P. Allongue, E. Souteyrand, J. Electroanal. Chem. 362 (1993) 79.
- [11] A.A. Pasa, W. Schwarzacher, Phys. Status Solidi A 173 (1999) 73.
- [12] A. Reitzle, F.U. Renner, T.L. Lee, J. Zegenhagen, D.M. Kolb, Surf. Sci. 576 (2005) 19.
- [13] D.M. Smilgies, R. Feidenhans'l, G. Scherb, D.M. Kolb, A. Kazimirov, J. Zegenhagen, Surf. Sci. 367 (1996) 40.
- [14] G. Scherb, D.M. Kolb, J. Electroanal. Chem. 396 (1995) 151.
- [15] P.M. Vereecken, K. Strubbe, W.P. Gomes, J. Electroanal. Chem. 433 (1997) 19.
- [16] R.M. Stiger, S. Gorer, B. Craft, R.M. Penner, Langmuir 15 (1999) 790.
- [17] B. Rashkova, B. Guel, R.T. Ptzschke, G. Staikov, W.J. Lorenz, Electrochim. Acta 43 (1998) 3021.
- [18] H. Nakano, K. Nakahara, S. Kawano, S. Oue, T. Akiyama, H. Fukushima, J. Appl. Electrochem. 32 (2002) 43.
- [19] P.J. Flanders, J. Appl. Phys. 63 (1988) 3940.
- [20] R. Meckenstock, O. von Geisau, J.A. Wolf, J. Pelzl, J. Appl. Phys. 77 (1995) 6439.